The reorder of trapped ions caused by background gas collisions

ZENGLI BA

Background gas collisions can result in reorder of the trapped ions designed for quantum computation, which is a problem for the information processing. Using the Monte Carlo simulation method, we estimate the reorder probability of each collision based on the distribution of background gas velocity. Comparing the result to the simplified energy barrier model, we give a more practical reorder probability lower than 40% at high radial trapping frequencies for a Ca^+ chain with up to 4 ions.

1. INTRODUCTION

Quantum computation has a promising future. For certain tasks, a quantum computer is superior to a classical computer because it can use superposition and entanglement for calculation. Among all the systems for practical quantum computing, trapped ions are one of the most advanced. However, when it comes to the actual application, trapped ions can meet with unexpected perturbations. Even in a ultra-high vacuum environment, there is still some gas remnant in the chamber. Collisions between ions and the gas molecules with thermal motion lead to two main defects. First is the position exchange of the ions, and the second is the destruction of the quantum state. Few studies have been done on this phenomenon, but it is not negligible when the operation time of the quantum computer comes to hours and even days. In this research, we mainly discuss the first sort of defect, the reorder caused by the background gas collision.

2. THEORETICAL ANALYSIS AND NUMERICAL SIMULATION

In the scale of atomic collision, we use a simplified semi-classical model instead of considering quantum scattering rigorously to avoid complicated calculation. Also we only take H_2 into account as the remnant of other gases can be omitted in the high vacuum chamber used in ion traps.

2.1 The Maxwell-Boltzmann distribution of the background gas

At room temperature, the speed and velocity of the background gas obey the Maxwell-Boltzmann distribution. On every dimension, the velocity of a background gas molecule, a vector which can be both positive and negative, has the distribution

$$f(v_i)dv_i = (\frac{m}{2\pi kT})^{1/2} e^{-\frac{mv_i^2}{2kT}} dv_i \,, \tag{1}$$

where m is the mass of the molecule, T is the temperature, and k is the Boltzmann constant. Since the distribution on each dimension is independent, by multiplying the distribution function together, we can get the 3D velocity Maxwell-Boltzmann distribution

$$f(\vec{v})d\vec{v} = f(v_x, v_y.v_z)dv_x dv_y dv_z = (\frac{m}{2\pi kT})^{3/2} e^{-\frac{m(v_x^2+v_y^2+v_z^2)}{2kT}} dv_x dv_y dv_z \,. \tag{2}$$

Considering speed $v = |\vec{v}|$, a scalar, we integrate Eq. (2) in the spherical coordinates and get the 3D speed distribution

$$f(v)dv = (\frac{m}{2\pi kT})^{3/2} \int_0^{2\pi} d\varphi (\int_0^{\pi} v^2 \sin\theta e^{-\frac{mv^2}{2kT}} d\theta) dv = (\frac{m}{2\pi kT})^{\frac{3}{2}} 4\pi v^2 e^{-\frac{mv^2}{2kT}} dv \,. \tag{3}$$

Integrating in the polar coordinates, the 2D speed distribution is

$$f(v)dv = (\frac{m}{2\pi kT}) 2\pi v e^{-\frac{mv^2}{2kT}} dv \,. \tag{4}$$

Similarly, the 1D speed distribution is

$$f(v)dv = (\frac{m}{2\pi kT})^{\frac{1}{2}} 2 e^{-\frac{mv^2}{2kT}} dv \,. \tag{5}$$

Fig. 1 shows the 1D, 2D and 3D probability density function of Maxwell-Boltzmann distribution. The most probable speed increases with the dimension.

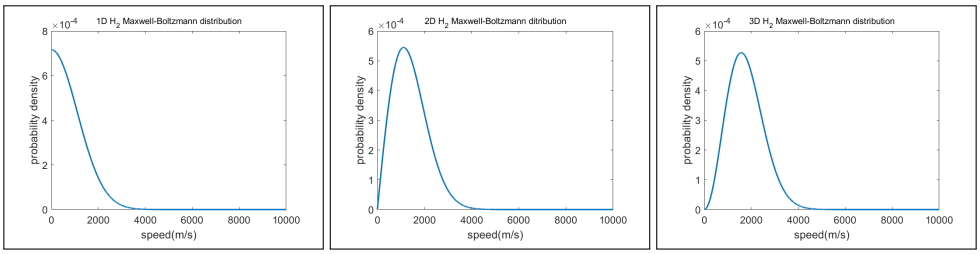

Fig. 1. Maxwell-Boltzmann probability density function. (a) The probability density function of 1D H_2 molecules at 300K. (b) The probability density function of 2D H_2 molecules at 300K. (c) The probability density function of 3D H_2 molecules at 300K.

2.2 The semi-classical collision model

We consider the interaction between the ion and the molecule to be a model of dipole moment interacting with a point charge, the trapped ion as a point charge and the molecule with a dipole moment induced by the point charge. This interaction potential has the form [1]

$$U(r) = -\frac{C_4}{r^4}\,, \tag{6}$$

where $C_4 = \frac{\alpha Q^2}{8\pi\varepsilon_0}$, α being the polarizability of the molecule and Q being the charge of the ion. The effective collision energy is

$$E = E_k - E_C = \frac{\mu v^2}{2}\,, \tag{7}$$

where E_C is the kinetic energy of the mass center in the two body system, E_k is the initial kinetic energy of the two bodies and $\mu = \frac{m_1 m_2}{m_1+m_2}$ is the reduced mass of the system, m_1 being the mass of the H_2 molecule and m_2 being the mass of a single ion. As the collision is transient, the potential of the trap is excluded.
The critical impact parameter of the ion-molecule collision is

$$b_c = (4C_4/E)^{-4}\,. \tag{8}$$

Then the Langevin cross section of the ion-molecule collision is

$$\sigma_L = \pi b_c^2 = \pi\sqrt{\frac{\alpha Q^2}{\pi\varepsilon_0\mu v^2}}\,, \tag{9}$$

and thus the collision rate $\gamma = nv\sigma_L$ can be calculated as

$$\gamma = \frac{pQ}{kT}\sqrt{\frac{\pi\alpha}{\mu\varepsilon_0}}\,, \tag{10}$$

according to the ideal gas equation $p = nk_BT$, where p is the pressure of the H_2 and n is the density of H_2 molecules. For given ions, molecules, and temperature, the collision rate γ is determined by the vacuum level.

However, due to the distribution of the molecule speed and the collision angle, not every collision is doomed to result in ion reorder and we managed to figure out that probability by modeling and simulation.

2.3 The kinetic energy transmitted in the collision

For the 1D collision, given two mass point m_1 and m_2 with initial velocity $\vec{u}$ and 0, the velocity after collision of m_1 and m_2 is

$$\vec{v_1} = \frac{m_1 - m_2}{m_1 + m_2}\vec{u},\ \vec{v_2} = \frac{2m_1}{m_1 + m_2}\vec{u}\,. \tag{11}$$

The 2D condition is more complex due to the distribution of incident angle. When thinking of the collision in a plane, we have to take the radius of two bodies into account. Here we consider two rigid balls m_1 and m_2 whose radius are r_1 and r_2, as is shown in Fig. 2(a), with initial velocity $\vec{u}$ and 0. Since the direction of impulse $\vec{I}$ points from the center of m_1 to m_2, the final velocity of m_2 is also in this direction. The collision angle β is defined as the angle between $\vec{u}$ and$\vec{I}$. In the position space, the vertical distance d is evenly distributed in the random collisions. In other words, $\sin\beta = d/(r_1 + r_2)$ is evenly distributed in the range of $[-1, 1]$. Parameters after the collision are defined in the Fig. 2(b), where the final velocity of m_1 and m_2 is $\vec{v_1}$ and $\vec{v_2}$.

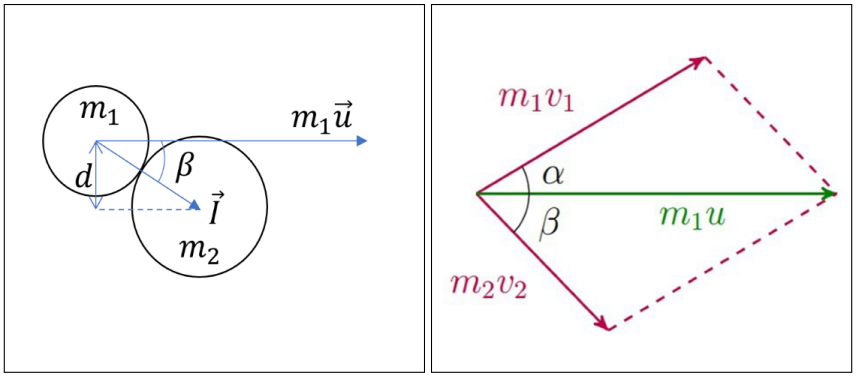

(a) (b)

Fig. 2. The 2D collision of two rigid balls. (a) The moment two rigid ball m_1 and m_2 collide. $\vec{u}$ is the initial velocity of m_1, $\vec{I}$ in the impulsion vector, *beta* is the collision angle and $d = (r_1 + r_2)\sin\beta$. (b) The vector parallelogram of the momentum of m_1 and m_2 after the collision.

According to the conservation of momentum, we have

$$m_1 u = m_1 v_1 \cos\alpha + m_2 v_2 \cos\beta \,, \tag{12}$$

$$0 = m_1 v_1 \sin\alpha + m_2 v_2 \sin\beta \,. \tag{13}$$

According to the conservation of energy, we have

$$\frac{1}{2} m_1 u^2 = \frac{1}{2} m_1 v_1^2 + \frac{1}{2} m_2 v_2^2 \,. \tag{14}$$

In order to deal with the Eq. (12) and Eq. (13), we consider the triangle of momentum and have

$$\frac{m_1 v_1}{\sin\beta} = \frac{m_2 v_2}{\sin\alpha} = \frac{m_1 u}{\sin(\alpha+\beta)} \,. \tag{15}$$

The final velocity can then be expressed as

$$v_1 = \frac{u\sin\beta}{\sin(\alpha+\beta)}, \; v_2 = \frac{m_1 u \sin\alpha}{m_2 \sin(\alpha+\beta)} \,. \tag{16}$$

Substituting Eq. (16) into Eq. (14), we come to a trigonometric equation

$$\sin^2(\alpha+\beta) = \sin^2\beta + \frac{m_1}{m_2}\sin^2\alpha \,. \tag{17}$$

After some mathematical operation,

$$\sin^2(\alpha+\beta) = \sin^2\beta(\sin^2\alpha + \cos^2\alpha) + \frac{m_1}{m_2}\sin^2\alpha \,,$$

$$\tan\alpha = \frac{\sin 2\beta}{\frac{m_1}{m_2} - \cos 2\beta} \,,$$

given β, the collision angle of m_2, then the scattering angle of m_1 is

$$\alpha = \text{acrtan}\frac{\sin 2\beta}{\frac{m_1}{m_2} - \cos 2\beta}\,, \tag{18}$$

and the proportion of energy transmitted from m_1 to m_2 is

$$\eta = \frac{\frac{1}{2}m_2 v_2^2}{\frac{1}{2}m_1 u^2} = \frac{4m_1 m_2}{(m_1+m_2)^2}\cos^2\beta\,. \tag{19}$$

In the actual 3D space, every collision can be described in the plane defined by $\vec{u}$ and $\vec{I}$ thus reduced to 2D conditions, so the energy transmission efficiency $\eta = \frac{4m_1m_2}{(m_1+m_2)^2}\cos^2\beta$ satisfies both situations. And the expectation of η is

$$\langle\eta\rangle = \langle\frac{4m_1m_2}{(m_1+m_2)^2}(1-\sin^2\beta)\rangle = \frac{8m_1m_2}{3(m_1+m_2)^2}\,, \tag{20}$$

as $\sin\beta$ has a continuous uniform distribution in $[-1,1]$.

2.4 A simplified energy barrier explanation

One way to calculate the probability of reorder after each collision is to define an energy barrier. Once the energy transmitted in the collision is over that barrier, the ions are considered to reorder. Take two ions for instance. In a linear harmonic trap with radial frequency f_r and axial frequency f_z, where f_r is greater than f_z, the energy of the system in equilibrium is

$$U_1 = \frac{1}{2}m(\omega_z^2(\frac{l_1}{2})^2\times 2) + \frac{Q^2}{4\pi\epsilon_0 l_1}\,. \tag{21}$$

Ions are aligned along z axis, m is the mass of a single ion and $l_1 = (\frac{Q^2}{2m\omega_r^2\pi\epsilon_0})^{\frac{1}{3}}$, which makes U_1 at its minimum if taken as a function of l_1. The energy of the barrier is complex to calculate accurately but Jungsang Kim's research proposed a method to estimate it [1]. The transition state is regarded to be the situation where two ions are aligned along a certain radial axis symmetrically, such as x axis. The energy is then expressed as

$$U_2 = \frac{1}{2}m(\omega_x^2(\frac{l_2}{2})^2\times 2) + \frac{Q^2}{4\pi\epsilon_0 l_2}\,, \tag{22}$$

where $l_2 = (\frac{Q^2}{2m\omega_z^2\pi\epsilon_0})^{\frac{1}{3}}$, making U_2 at its minimum if taken as a function of l_2. The energy barrier is then defined as

$$\Delta U = U_2 - U_1\,. \tag{23}$$

Fig. 3(a) shows the energy barrier calculated based on the method mentioned above for different

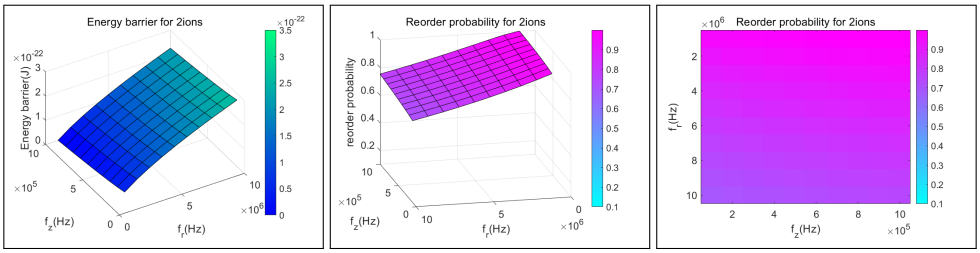

(a) (b) (c)

Fig. 3. The simplified calculation of energy barrier and reorder probability. (a) The energy barrier calculated with Eq. (23) for two Ca^+ ions. (b)(c) The reorder probability calculated by Eq. (25) for two Ca^+ ions in the 3D space. The result is higher than 70% in the linear harmonic with radial frequency 1-10MHz and axial frequency 0.1-1.0MHz.

trapping frequencies. In an ion trap designed for calcium, we denote the mass of H_2 and Ca^+ as

m_1 and m_2. The average energy transmitted to the ion was claimed to be $\langle E_{Ca^+} \rangle = \frac{2m_1m_2}{(m_1+m_2)^2} E_{H_2}$ [1, eqn. (5)](annotation: this is completely correct only when the angle β in [1] is distributed evenly in the range of $[-\pi/2, \pi/2]$, which is not the actual case as discussed above. But it anyway has the correct magnitude and only has a different coefficient compared to Eq. (20), regardless of the slight difference of collision model between section 2.2 and section 2.3)
The critical velocity of H_2 can then be expressed by the reorder energy barrier

$$v_p = \frac{1}{m_1}\sqrt{\frac{(m_1+m_2)^2\Delta U}{2m_2}}\,. \tag{24}$$

In general, the incident molecules with speed less than v_p will not lead to reorder while those greater than v_p will result in reorder. Combining the Maxwell-Boltzmann speed distribution Eq. (3)-(5), the reorder probability of each collision is

$$p = \int_{v_p}^{\infty} f(v)dv\,, \tag{25}$$

where $f(v)$ is the probability density function.
Specially, for the 3D position space, $p = \int_{v_p}^{\infty} (\frac{m}{2\pi kT})^{\frac{3}{2}} 4\pi v^2 e^{-\frac{mv^2}{2kT}} dv$. The calculated reorder probability in Fig. 3(b) and 3(c) of two Ca^+ ions in the trap is basically over 70%, with trapping frequencies f_r in the interval of 1-10MHz and f_z in the interval of 0.1-1.0MHz, which indicates that reorder is inevitable in most collisions, according to this simplified analysis.

2.5 The Monte Carlo simulation method

Although we can have some overview of the energy transmitted during the collision through the concept of η on average, the distribution of velocity should not be overlooked especially when it is nonlinear. In order to have a better understanding of the detailed dynamics, we use a series of samples of H_2, whose velocity is produced randomly with the probability density function discussed in section 2.1 to simulate the actual collision and the proportion of reorder times versus the overall collision samples is regarded as the reorder probability, which is known as the Monte Carlo simulation, as long as the amount of samples is adequate according to the *central limit theorem* in probability theory.
First, we need the samples of velocity of H_2. Comparing the distribution of velocity on each dimension in Eq. (1) with the normal distribution

$$f(x) = \frac{1}{\sigma\sqrt{2\pi}} e^{-\frac{(x-\mu)^2}{2\sigma^2}}\,, \tag{26}$$

we find it has the same form as normal distribution with $\mu = 0$, $\sigma = \sqrt{\frac{kT}{m}}$. We are able to attain the random velocity variables v_x, v_y and v_z with such distribution directly using the normal distribution function from most programming library. By assembling these velocities, we have the samples of speed in 1D, 2D, and 3D space respectively, $v_{1D} = |v_x|$, $v_{2D} = \sqrt{v_x^2 + v_y^2}$ and $v_{3D} = \sqrt{v_x^2 + v_y^2 + v_z^2}$. Fig. 4 shows the proportion of samples produced(diamond) that accord with the analytical probability density(dashed) correspondingly. In a similar way, we express the velocity of the incident H_2 molecule as $\vec{v}_{H_2} = (v_x, v_y, v_z)$.

Second, with the incident H_2 molecule, we need to give the the velocity transmitted to Ca^+ in each collision. Since every collision is an independent event, we simulate every single collision and repeat this procedure. We use the ion-molecule interaction potential to discuss the collision rate in section 2.2, but for each collision happening, we approximate the Ca^+ ion and the H_2 molecule to be two rigid balls to simplify the calculation. $\vec{r}$ is defined as the position vector pointing from the center of H_2 to Ca^+ the moment they touch and the impulse vector is along this direction as well, thus the motion of two balls confined in the plane determined by $\vec{r}$ and $\vec{v}_{H_2}$. Since $\vec{r}$ is evenly distributed in every direction in the position space independent to $\vec{v}_{H_2}$, we can produce the samples of two random variables respectively. The base vector in the collision plane can then be expressed with $\vec{r}$ and $\vec{v}_{H_2}$

$$\hat{x'} = \frac{\vec{v}_{H_2}}{v_{H_2}},\ \hat{y'} = \frac{\vec{r} - (\vec{r}\cdot\hat{x'})\hat{x'}}{|\vec{r} - (\vec{r}\cdot\hat{x'})\hat{x'}|}. \tag{27}$$

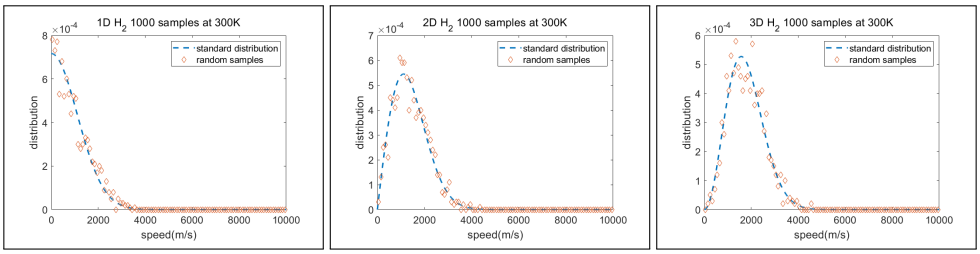

(a) (b) (c)

Fig. 4. 1000 samples of speed of H_2 molecules at 300K. (a) Speed samples produced for 1D space by random number. (b)(c) Samples in 2D and 3D space. Dashed line is the analytical probability density function and diamonds are count of samples in the neighbourhood divided by 1000. The 1000 samples basically obey the standard Maxwell-Boltzmann distribution.

In this way, we are able to simplify the 3D collision to a collision in the $x' - y'$ plane and get the final result via the transformation of coordinates. As for the 2D situation discussed in section 2.3, the vertical distance d in Fig. 2(a) is evenly distributed in the position space. Thus we have, for the collision angle β, $\sin\beta$ obeys the continuous uniform distribution in $[-1, 1]$. Using the standard function in library, we produce such variable d'. Since $d' = \sin\beta$, the random variable β can be expressed by $\beta = \arcsin(d')$ based on the continuous uniform distribution. The velocity of Ca^+ ion after the collision can be expressed with the base vectors $\hat{x'}$ and $\hat{y'}$

$$\vec{v}_{Ca^+} = \frac{2m_1}{m_1 + m_2} v_{H_2} \cos\beta(\cos\beta\hat{x'} + \sin\beta\hat{y'}) \,. \tag{28}$$

Finally, we need to determine the time evolution of the collided Ca^+ ion together with rest of the ions. The force Ca^+ ions feel consists of the trapping force and the Coulomb's repulsion between the ions. The position vector being the function of time, we use the Euler method

$$\vec{a}_i(t) = -\nabla Q U(\vec{r}_i(t)) + \sum_{j \neq i} \frac{Q^2}{4\pi\varepsilon_0} \frac{\vec{r}_{ji}(t)}{r^3_{ji}(t)} \,, \tag{29}$$

$$\vec{v}_i(t + \Delta t) = \vec{v}_i(t) + \vec{a}_i(t)\Delta t \,, \tag{30}$$

$$\vec{r}_i(t + \Delta t) = \vec{r}_i(t) + \vec{v}_i(t + \Delta t)\Delta t \,, \tag{31}$$

where U is the electric potential of the trap, Δt is the time step set for calculation and $\vec{r}_{ji}(t)$ is the position vector pointing from the ion j to the ion i at the time t, to give the numerical solution to this second-order differential equation. Fig. 5(a) shows the simulation via this method, where the 2 Ca^+ ions are confined in an ideal harmonic trap with radial frequency 5MHz and axial frequency 0.2MHz and the velocity of ion2 is set to be $\vec{v}_{Ca^+}$ =(5m/s,0,5m/s) with time step Δt = 1ns. Considering the z coordinates of the 2 ions, they do not exchange the positions in the 2-ion chain in this condition.

As for formula (31) that is designed to calculate the position vector for the next step, we do not adopt another apparent expression which has a better local truncation error,

$$\vec{r}_i(t + \Delta t) = \vec{r}_i(t) + \frac{\vec{v}_i(t) + \vec{v}_i(t + \Delta t)}{2} \Delta t \,, \tag{31'}$$

because formula (31) usually has a greater area of numerical stability than formula (31'), namely, the latter easier to diverge with time. Fig. 5(b) and 5(c) illustrate the stability of two numerical method formula (31) and (31') respectively in the same condition as Fig. 5(a) and formula (31) gives a much more stable numerical solution, which is in agreement with our expectation.

For the complete procedure of Monte Carlo simulation, we have the following procedures.
1. Produce a group of 1000 samples of the incident velocity of H_2 molecule which obeys the Maxwell-Boltzmann distribution.
2. For each sample of the incident H_2, calculate the velocity of the Ca^+ ion $\vec{v}_{Ca^+}$ after the collision according to Eq. (28).

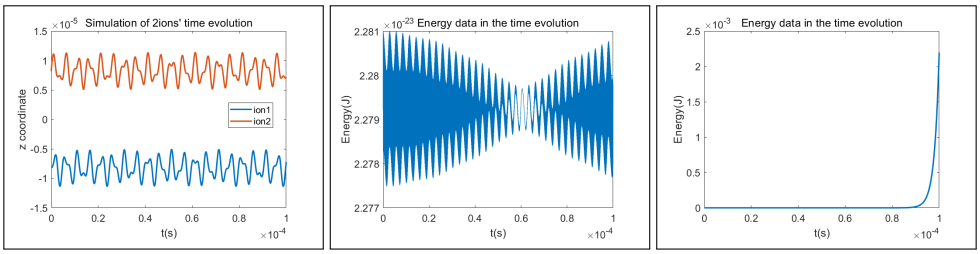

(a) (b) (c)

Fig. 5. (a) The simulation of time evolution for two Ca^+ ions in the harmonic trap with radial frequency 5MHz and axial frequency 0.2MHz using the Euler method. Ion2 has the initial velocity (5m/s,0,5m/s). (b) The total energy of the ions during the time evolution in the same given condition and the solution is convergent. (c) The total energy of the ions during the time evolution using formula (31') in the same given condition and the solution diverges.

3. Simulate the time evolution of every ion in the trap with the Euler method, formula (29)-(31). If there is an exchange of axial z coordinates of the ion chain, this sample is defined to have reorder. For 2 ions in the Fig. 5(a), if the z coordinate of ion1 is greater than ion2 in a period of time, reorder is considered to happen.
4. Calculate the proportion of samples having reorder and the value is the estimated probability in the simulation.

2.6 Monte Carlo simulation of ions in ideal harmonic potential trap

We first simulate on the ions in an ideal harmonic trap with such potential

$$U = \frac{1}{2}m\omega_z^2 z^2 + \frac{1}{2}m\omega_r^2(x^2+y^2)\,, \tag{32}$$

which is not practical for the real electric potential according to the *Earnshaw'stheorem*. We start with the 2D condition, so the ions are confined in the $x-z$ plane and only two dimensions are considered for the Maxwell-Boltzmann distribution of H_2. For the simulation, the number of samples of incident H_2 is 1000 and the evolution time is 0.1ms with $\Delta t = 1$ns for each step.The radial trapping frequency f_r is 1-10MHz, while the axial frequency f_z is 0.2-1.0MHz. The reorder probability for 2D two ions is shown in Fig. 6(a). After taking y direction into account, we produce the 3D distribution of H_2 and the simulation is shown in Fig. 6(b).

Fig. 6(c) shows the different reorder probability of 2D and 3D simulations with a fixed axial frequency 0.2MHz. Comparing the two situations, we find the 3D has a higher reorder probability about 10% more than the 2D. This is because with the increase of dimension, the incident H_2 molecule has more degree of freedom as well as a high average kinetic energy, thus the Ca^+ ions likely to acquire more energy from the collision and to reorder more frequently. Since the third degree of freedom can not be overlooked, despite the motion on x direction and y direction are equivalent, we base our simulation on the 3D case. Fig. 6(d) and 6(e) show the simulated reorder probability for 3 ions and 4 ions in the ideal harmonic potential respectively.

Comparing the simulation result of different ions in the same plot, we find that the reorder probability is slightly lower for 2 ions when the radial frequency in no more than 6MHz and there is no big difference when the radial frequency is higher than 6MHz, according to Fig. 6(f) where the axial frequency is set unchanged at 0.4MHz.

We also compare the effect of collisions on different ions. For 3 ions, the collision probability is approximately $\frac{1}{3}$ for the central ion and $\frac{2}{3}$ for side ions and the reorder probability in 2D simulation is shown in Fig. 7(a). Similarly for 4 ions, the collision probability is approximately $\frac{1}{2}$ for the central ions and $\frac{1}{2}$ for side ions and the reorder probability in 2D simulation is shown in Fig. 7(b). Although the reorder probability of collisions on the side ion is generally lower than the central ion, there is no big difference between collisions on central and side ions for the ion chain with up to 4 ions according to Fig. 7. However, the difference probably increases with the number of ions in the chain.

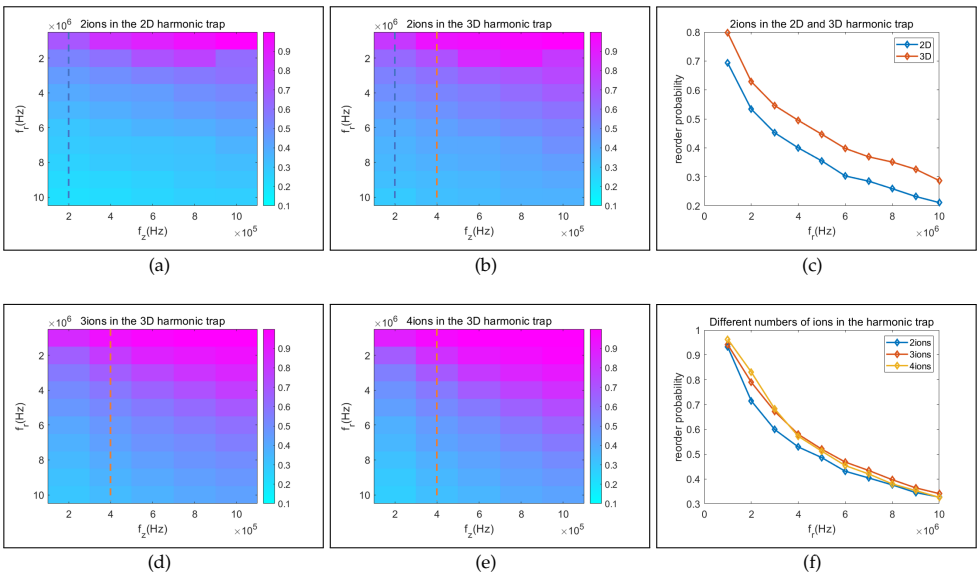

Fig. 6. Simulation result of ions in the harmonic trap (a) The result of 2 ions in the 2D harmonic trap. (b) The result of 2 ions in the 3D harmonic trap. (c) The comparison of 2D and 3D result along the blue dashed line in (a) and (b) shows the 3D result has a higher reorder probability. (d)(e) The result of 3 and 4 ions in the 3D harmonic trap. (f) The comparison of 2, 3, and 4 ions' result along the orange dashed line in (b)(d)(e). The reorder probability is lower than 50% for all situations when radial frequency higher than 6MHz.

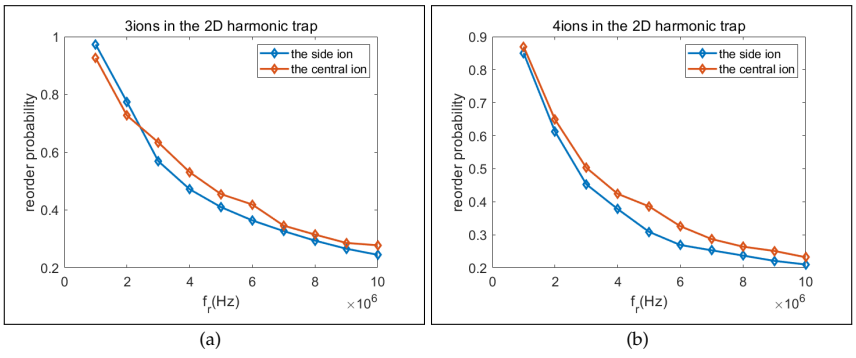

Fig. 7. Discussion on different ions collided. (a) 3 ions in the 2D harmonic trap with collisions on the central and the side ion respectively. (b) 4 ions in the 2D harmonic trap with collisions on the central and the side ion respectively. The collisions on side ions are basically less likely to cause reorder.

2.7 Comparison to previous work

One phenomenon remarkable is that the reorder probability in the simulation is much lower than the theoretical result in section 2.4 according to Kim [1].

To explain this, we use a rough approximation to demonstrate the defect of the model introduced in section 2.4. We set ion2 static at the initial position and give the distribution of electric potential energy in the space for ion1 in Fig. 8(a).As is shown in in Fig. 8(b), there is a red dotted saddle point in such potential which is the local maximum along the z direction while the local minimum along the radial direction. We calculate the energy difference between the saddle point and the ground state and show the result in Fig. 8(c). As is shown in Fig. 8(d), we compare the result to energy barrier in section 2.4 Fig. 3(a) and find it is close to the energy barrier defined in the previous APL paper. The fact that ion2 is also moving and thus the energy of the saddle point should be lower account for the excess compared to the result in section 2.4. This rough approximation vividly explain that the barrier calculated in formula (23) is the simply lowest barrier and has overestimated the reorder probability because the path for ion1 to overcome the energy saddle is not necessarily the lowest, but determined by the collision of incident H_2. Thus, the simulation result acquired by Monte Carlo method is closer to the actual situation.

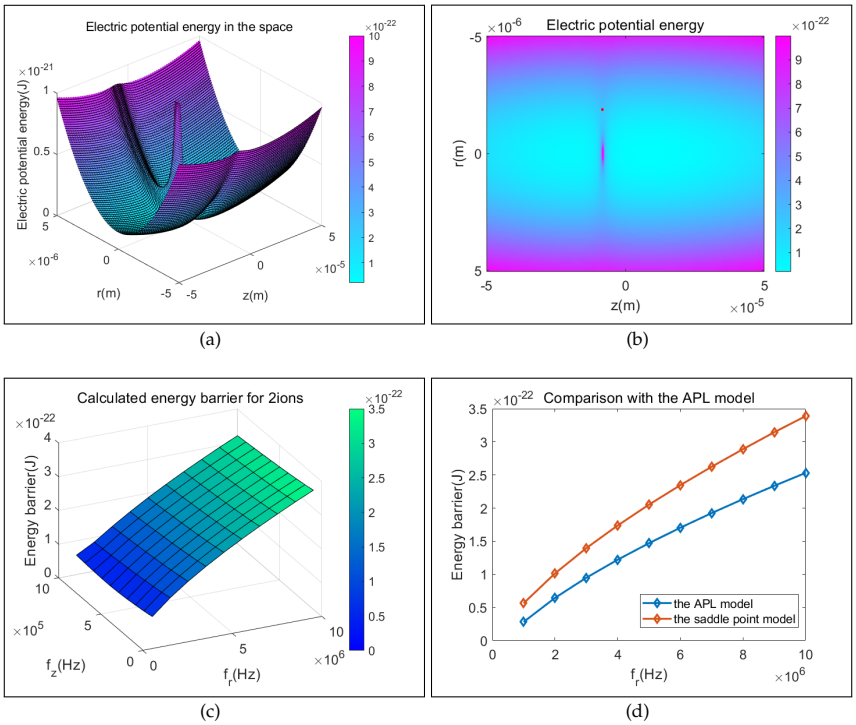

Fig. 8. Discussion on the energy barrier model. (a) The potential energy of a Ca^+ ion in the electric field that consists of a harmonic trap with the radial frequency 5MHz and the axial frequency 0.2MHz and a static positive point elementary charge. (b) The plan view of (a) illustrates a saddle point(red dotted) in the potential, which is the local minimum along the radial direction. (c) The energy difference between the saddle point and the global minimum for the Ca^+ ion. (d) Comparison of two results in the APL model in Fig. 3(a) and approximate saddle point model at a static axial frequency 0.4MHz and they are very close.

2.8 Monte Carlo simulation of ions in ideal pseudo potential trap

The 3D linear pseudo potential consists of a rf electric potential and a static electric potential, which has a form

$$\varphi = V\cos(\Omega t)\frac{x^2-y^2}{r_0^2} + U\frac{2z^2-x^2-y^2}{2z_0^2} \tag{33}$$

where V is used to describe the amplitude of the rf potential, U is the parameter of the static potential and Ω is the driving radio frequency. For an ion in this potential the force is

$$\vec{F} = -\nabla(Q\varphi) = \frac{2QV\cos(\Omega t)}{r_0^2}(-x, y, 0) + \frac{QU}{z_0^2}(x, y, -2z) = \vec{F}_{rf}\cos(\Omega t) + \vec{F}_{dc} \,. \tag{34}$$

Based on the pseudo-potential approximation, averaging the force the ion feels during a rf period, we have a effective potential for the ion

$$U_{eff} = \frac{Q^2}{4m\Omega^2}|\vec{E_{rf}}|^2 + Q\varphi_{dc} = (\frac{Q^2V^2}{m^2\Omega^2r_0^4} - \frac{QU}{2z_0^2})(x^2 + y^2) + \frac{QU}{z_0^2}z^2 \,, \tag{35}$$

as if it were in a harmonic potential [3].(annotation: this result is different from [3, eqn. (2.48)] with a factor 4 . Formula (35) is proved to be correct and there is a factor 4 found to be left out in [3, eqn. (2.32)], based on both theoretical calculation and simulation on Paul traps.) Analogy to the standard harmonic potential, we have the effective radial and axial frequency of the trap

$$k_r = 2(\frac{Q^2V^2}{m^2\Omega^2r_0^4} - \frac{QU}{2z_0^2}),\ \omega_r = \sqrt{\frac{2Q^2V^2}{m^2\Omega^2r_0^4} - \frac{QU}{mz_0^2}} \,, \tag{36}$$

$$k_z = \frac{2QU}{z_0^2},\ \omega_z = \sqrt{\frac{2QU}{mz_0^2}} \,. \tag{37}$$

According to Wolfgang Paul [2], the stability of this pseudo-potential trap is influenced by two critical parameters

$$q \equiv \frac{4QV}{m\Omega^2r_0^2},\ a \equiv \frac{4QU}{m\Omega^2r_0^2} \,, \tag{38}$$

which actually dominate the existence of solution of the Mathieu differential equation.

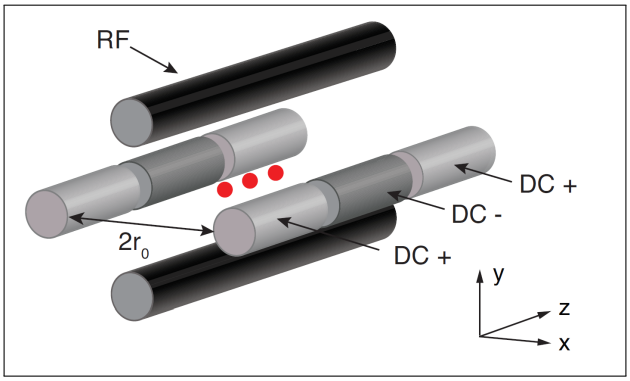

Fig. 9. The sketch of a rf Paul trap from [3]. Red dots are trapped ions and the four electrodes are conneted to both dc and ac voltage.

To realize such pseudo-potential in the experimental set up, we utilize the quadrupole trap, which is also known as the Paul trap. A sketch of the Paul trap [3] is shown in Fig. 9, with the dc voltage providing the static potential and ac voltage providing the rf potential. In the ideal condition, assuming the cylindrical electrodes to be infinitesimal in radius and infinite in length, we can get the analytical solution of electric potential in the space that accords with the theory of pseudo-potential. Focusing on the effect of the ac voltage, in the coordinates in Fig. 9, the potential of the four electrodes is

$$\varphi_{Paul} = V\cos(\Omega t)(x^2 - y^2),\ for\ x = \pm r_0,\ y = \pm r_0 \,. \tag{39}$$

Taking Eq. (39) as the boundary conditions, in the rest of the entire space, the electric potential obeys the Laplace's equation

$$\nabla^2\varphi_{Paul} = 0,\ for\ (x^2, y^2) \neq (r_0^2, r_0^2) \,. \tag{40}$$

A trial solution can be found

$$\varphi_{Paul} = V\cos(\Omega t)\frac{x^2 - y^2}{r_0^2}\,. \tag{41}$$

According to the *uniqueness theorem* in electromagnetism, formula (41) which is in the perfectly same form as the ac part of the ideal pseudo-potential, is the only solution to Eq. (39) and Eq. (40). For practical use, ions are confined around the center of the trap and the distance to the electrodes is much greater than the radius of the electrodes, so the approximation stated above is reasonable and the Paul trap is proved to be an effective way to produce a harmonic pseudo potential.

To simulate the motion of ions in the pseudo potential, we set the parameter q which is defined in Eq. (38) a constant 0.3034 to ensure the motion in the trap has a stable solution. Given effective trapping frequency ω_r and ω_z, according to Eq. (34)-(37), the force exerted on ions by the trap is

$$\vec{F}_{trap} = m\frac{\omega_r^2 + \omega_z^2/2}{q/4}\cos(\Omega t)(-x, y, 0) + m\omega_z^2(\frac{x}{2}, \frac{y}{2}, -z)\,, \tag{42}$$

where $\Omega = \frac{2\sqrt{2\omega_r^2+\omega_z^2}}{q}$, according to Eq. (36)-(38).

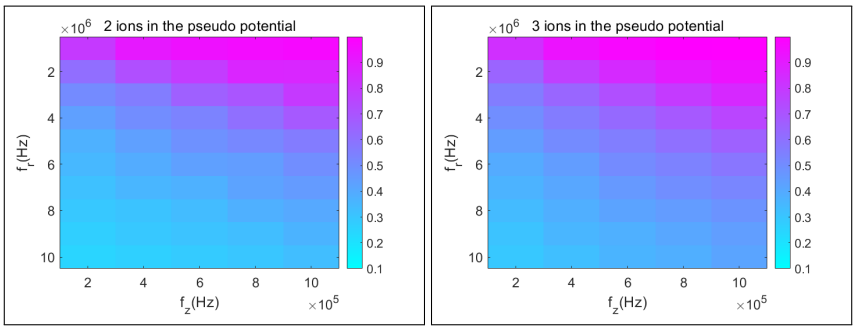

(a) (b)

Fig. 10. Simulation result of ions in the pseudo potential. (a) 2 ions in the pseudo-potential. (b) 3 ions in the pseudo-potential. The result is in agreement with the 3D harmonic trap.

Fig. 10 shows the simulation result of 2 ions and 3 ions in the pseudo-potential trap. We find the reorder probability agree well with the result of ions in the harmonic trap in Fig. 6(b) and Fig. 6(d), which proves that the pseudo-potential exerts an effective force on the ions very close to the harmonic trap and that the simulation result in 3D harmonic trap is sufficient to the further study on the actual linear Paul trap.

3. CONCLUSION AND OVERLOOK

In this paper, we studied the reorder of trapped ions cased by background gas collisions systematically. We followed Kim's idea of utilizing a simplified semi-classical model to understand the ion-molecule interaction and calculate the collision rate. Using the Monte Carlo method, we simulated the motion of Ca^+ ions both in the ideal harmonic trap and in the ideal pseudo-potential trap and estimated the reorder probability in each collision. Comparing our simulation result with Kim's calculation, we found a defect in his simplified energy barrier model and reached the result that the reorder probability can reduce to less than 40% for 2-4 Ca^+ ions if radial trapping frequency is around 8MHz. Despite of this, the background gas collisions are still an issue to be settled for long time quantum computing.

There are still many topics to study in the future. For example, the numerical calculation can be optimized using the Verlet method instead of the Euler method, the ion chain with tens of ions can be simulated to confirm the stability of the long chain in the collisions and the Hamiltonian mechanics can be adopted to search for a analytical solution in the phase space. Moreover, experiments can be designed to verify the estimated reorder probability in this paper. Some cooling methods can be applied to reduce the reorder rate ,thus further reducing the effects of collisions.

4. ACKNOWLEDGEMENTS

I want to thank Professor Sara Mouradian for providing me the opportunity to carry out my summer research at her group at University of Washington. Without her support and guidance, I would not have seized the chance to join the quantum calculation and ion trapping community and find such a meaningful research subject.

Moreover, I want to thank all members of the SQRLab group, Malek, Yuan, Duy and Katharine, especially Jacob and Ritika: for their generously offering the thesis and data on trap designing, without which I would not have got a good understading of the Paul trap.

REFERENCES

[1] Yuhi Aikyo, Geert Vrijsen, Thomas W. Noel, Alexander Kato, Megan K. Ivory, and Jungsang Kim , "Vacuum characterization of a compact room-temperature trapped ion system", Appl. Phys. Lett. 117, 234002 (2020).

[2] W. Paul, Electromagnetic traps for charged and neutral particles, Rev. Mod. Phys. 62, 531 (1990).

[3] G. Littich. Electrostatic Control and Transport of Ions on a Planar Trap for Quantum Information Processing. Master thesis, ETH Zurich and University of California, Berkeley(2011).